Author Query Form

Journal Title **:** Lupus (LUP)
Article Number **:** 355299

Dear Author/Editor,
Greetings, and thank you for publishing with SAGE. Your article has been copyedited and typeset, and we have a few queries for you. Please address these queries when you return your proof corrections. Thank you for your time and effort.

Please ensure that you have obtained and enclosed all necessary permissions for the reproduction of artistic works, (e.g. illustrations, photographs, charts, maps, other visual material, etc.) not owned by yourself, and ensure that the Contribution contains no unlawful statements and does not infringe any rights of others, and agree to indemnify the Publisher, SAGE Publications Ltd, against any claims in respect of the above warranties and that you agree that the Conditions of Publication form part of the Publishing Agreement.

Any colour figures have been incorporated for the on-line version only. Colour printing in the journal must be arranged with the Production Editor, please refer to the figure colour policy outlined in the e-mail.

Please assist us by clarifying the following queries:

1. Bottom of page 6: Citation of Figure 3 changed to Figure 5, as Figure 5 was note cited; if this is not correct please cite Figure 5 in the text retaining numerical order of citation.
2. Please provide citation for Table 4 and Table 7 in the text.
3. Please provide accessed date for reference 55.
4. Please provide reference 69 in reference list as it is cited in the text

Lupus (2009) 0, 1–14
http://lup.sagepub.com

PAPER

Sugar-free, glycine-stabilized intravenous immunoglobulin prevents skin but not renal disease in the MRL/lpr mouse model of systemic lupus

Z Racz[1], E Nagy[2], L Rosivall[1], J Szebeni[1] and P Hamar[1]
[1]Institute of Pathophysiology, Semmelweis Medical University, Nagyvarad ter 4., Budapest 1089, Hungary; and [2]Central Immunological Laboratory, Semmelweis Medical University, Mária u. 41., Budapest 1085, Hungary

Intravenous immunoglobulin (IVIG) has a therapeutic potential in many autoimmune diseases. Based on its immune modulating and complement inhibiting effects, IVIG has been tested in systemic lupus erythematosus (SLE), but due to osmotic tubular injury caused by immunoglobulin-stabilizing sugar components, lupus nephritis had been accelerated in some patients, thus IVIG use in SLE has been abandoned. The availability of non-sugar-stabilized IVIG raised the possible re-evaluation of IVIG for SLE. We investigated high-dose, long-term non-sugar-stabilized IVIG treatment on skin and renal SLE manifestations in the MRL/lpr mouse model. Animals were treated once a week with glycine-stabilized IVIG or saline (0.2 ml/10 g BW) from 6 weeks until they were humanely killed at 5 months of age. IVIG diminished macroscopic cutaneous lupus compared with saline treated mice. Histology and complement-3 immunostaining also demonstrated a significant reduction of skin disease after IVIG treatment. However, renal histology and function were similar in both groups. Compared with typical osmotic tubular damage induced by 5% sucrose and 10% maltose (used for IVIG stabilization), we did not observe any osmotic tubular injury in the glycine-stabilized IVIG treated mice. Our data demonstrate a beneficial effect of IVIG on skin lupus without renal side-effects. Deeper understanding of the organ-specific pathomechanism may aid an individualized SLE therapy. *Lupus* (2009) **0,** 1–14.

Key words: complement; intravenous immunoglobulin; lupus nephritis; osmotic nephrosis; skin; systemic lupus erythematosus

Introduction

Systemic lupus erythematosus (SLE) is one of the most common autoimmune diseases influencing about 0.5% of the population in Western countries.[1] Type III hypersensitivity with deposition of circulating immunocomplexes and consequent complement activation are thought to play a central role,[2] but the theory of uniform SLE pathology does not explain differences among patients in disease severity and organ manifestations, thus local factors or differential organ pathomechanisms have been suggested to determine disease outcome.[3,4]

Human SLE has a wide spectrum of clinical manifestations ranging from antiphospholipid syndrome without major organ involvement, through mild cutaneous lupus, more severe lupus nephritis, and fulminant, often lethal neurolupus.[5] The uniform theory of type III hypersensitivity with preformed immune complex deposition derived complement activation in innocent bystander organs[6] does not explain this wide spectrum of disease manifestation. Differential pathomechanisms of SLE organ manifestations have been suggested by many studies. Local factors such as VCAM-1,[7,8] thrombomodulin,[9] E-selectin,[10] neutrophil gelatinase-B(NGAL)/lipocalin-2,[11] natural killer T-cells,[12] oestrogen,[13] TNF-alpha,[14] IFN-gamma[4] and IL-12[15] have been demonstrated to differentially influence disease outcome in skin and kidney lupus. Genetic factors[16] such as CD1d,[17] beta(2)-microglobulin,[18] MHC class II (Ia)

Correspondence to: Péter Hamar, MD, PhD, Institute of Pathophysiology, Semmelweis University, Faculty of General Medicine, Budapest, Hungary Nagyvárad tér 4. H-1089 Budapest, Hungary. Email: hampet@net.sote.hu
Received 7 May 2009; accepted 26 October 2009

10.1177/0961203309355299

antigen,[19] Yaa gene[20] also seem to differentially alter organ-specific autoimmunity in mice. In accordance with these data, our present paper demonstrates differential involvement of skin and kidney in a mouse model.

At present, therapy for SLE is not specific and toxic.[21] To minimize side effects, the aim of modern SLE therapy is to regulate rather than suppress the immune response. One possible immune modulating agent is intravenous immunoglobulin (IVIG),[22] which may neutralize autoantibodies, bind complement and prevent the formation of membrane attack complex.[23] High-dose IVIG improved cutaneous lesions in autoimmune skin diseases, including lupus.[24] Remission of clinical symptoms, with decreased anti-DNA antibody levels, and increased total complement concentration was demonstrated in clinical trials.[25–27] IVIG (2 g/kg) is indicated in severe SLE cases[28,29] or in order to spare steroids or cyclophosphamide.[30,31]

However, IVIG nephrotoxicity can be a serious rare complication of high-dose (0.8–5 g/kg) IVIG therapy.[32–35] The exact mechanism of IVIG-associated acute renal failure (ARF) is still unclear. Renal histology demonstrates vacuolization and cellular swelling of proximal tubules, called osmotic nephrosis or hydropic degeneration.[36] Osmotic nephrosis, especially in the presence of risk factors (age >65 years, pre-existing renal insufficiency, diabetes, the concomitant use of other nephrotoxic agents, volume depletion),[37] may lead to ARF (estimated incidence or around 1%).[38–40] Nephrotoxicity appeared to be due to the sugar components[41] used to stabilize the tertiary structure of IgG in IVIG preparations.[42,43] Sucrose is assumed to have the most remarkable propensity to cause osmotic nephrosis.[44,45] In modern IVIG products the amino acid glycine is used instead of sugar stabilizers. Glycine is an intracellular component and has various pathways for its metabolic degradation. Sucrose-stabilized IVIG induced renal impairment, but this complication was absent when glycine-stabilized IVIG was used.[46]

Maltose-based IVIG therapy is also thought to be a safer alternative than using sucrose-based preparations, since maltase is present in the brush border of proximal convoluted tubules, it can be metabolized in renal tubules, unlike sucrose, and thus less tubular osmotic damage is expected.

The MRL/MpJ-*Fas*^{lpr} mouse (MRL/lpr) model of human SLE[47] is characterized by autoreactive lymphoproliferation and autoantibody production beginning at 8 weeks of age.[48] Severe glomerulonephritis develops, characterized by IgG deposition and inflammatory infiltration.[49,50] Skin lesions also mimic those of human lupus[51] characterized by immune complex and complement (mainly complement 3) deposition[52] with a predilectional site at the interscapular region, ears and nose.

We[3] and others[12] have recognized, that pregnancy[3] or immunoregulatory modifications[13] in the MRL/lpr mouse may differentially effect skin and kidney disease. Cytokine profile differences or invariant natural killer T-cell (NKT cell) regulation in the skin, but not in the kidney[17,18] were responsible for the organ-specific differences in disease activity. Thus, we investigated high-dose, long-term glycine-stabilized IVIG treatment in MRL/lpr mice to elucidate IVIG's mechanism of beneficial action and toxicity in SLE.

Results

Systemic administration of high-dose IVIG alleviated skin disease

In saline-treated control MRL/lpr mice skin lesions started to develop at the age of 3 months, in the interscapular region and ears as hair loss (alopecia) and scabs (scars). At the time they were humanely killed (at 5 months of age) ulceration and massive destruction were observed in all saline-treated animals. IVIG treatment strikingly reduced macroscopic skin and ear lesions at the time of death. In IVIG-treated animals only mild or no lesions were observed (Table 1). Microscopically, in saline-treated skins, the dermis was thickened and severe inflammation was present. Hyper- and/or parakeratosis, thickening and structural destruction (loss of the 'cobble-stone pattern') of stratum spinosum was also observed. These microscopic skin lesions were largely reduced or practically absent in IVIG-treated animals (Figure 1). Thickening, vacuolization and tortuosity of the basement membrane were also observed in samples with high scores (Table 1). Pathological changes of the basement membrane were twice as frequent in saline-treated control animals as in IVIG-treated mice (Table 1). Inflammatory infiltration by mononuclear cells (lymphocytes, plasma cells, monocytes, rarely eosinophils) was also significantly reduced in IVIG-treated animals. Plasma cells were observed in three samples of saline-treated controls but in none of the IVIG-treated mice (Table 1).

Overall skin score demonstrated a significant protection by IVIG treatment, as the total score of microscopic evaluation of the skin was reduced by IVIG by a factor of more than two.

Table 1 Skin disease: macroscopic and microscopic scores of intravenous immunoglobulin (IVIG) and saline-treated MRL/lpr mice

	IVIG (n = *8*)	*Saline* (n = *10*)	p-*value*
Macroscopic			
Skin	6 ± 0.866	13 ± 1.34	<0.03
Ear	2 ± 0.44	8 ± 0.78	<0.05
Microscopic			
Dermal thickening and inflammation	0.642 ± 0.47	1.212 ± 0.58	0.036
Basement membrane thickening	0.952 ± 0.2	0.415 ± 0.54	0.013
Hyper-and/or parakeratosis	0.659 ± 0.4	0.399 ± 0.68	0.328 (n.s.)
Stratum spinosum thickening	0.26 ± 0.33	0.67 ± 0.58	0.08
Loss of the cobble-stone pattern	2	0	–
Inflammatory infiltration	0.498 ± 0.7	0.753 ± 0.6	0.429 (ns.)
Infiltration by plasma cells	3	0	–
Overall score	221 ± 0.43	4.19 ± 0.623	0.0002

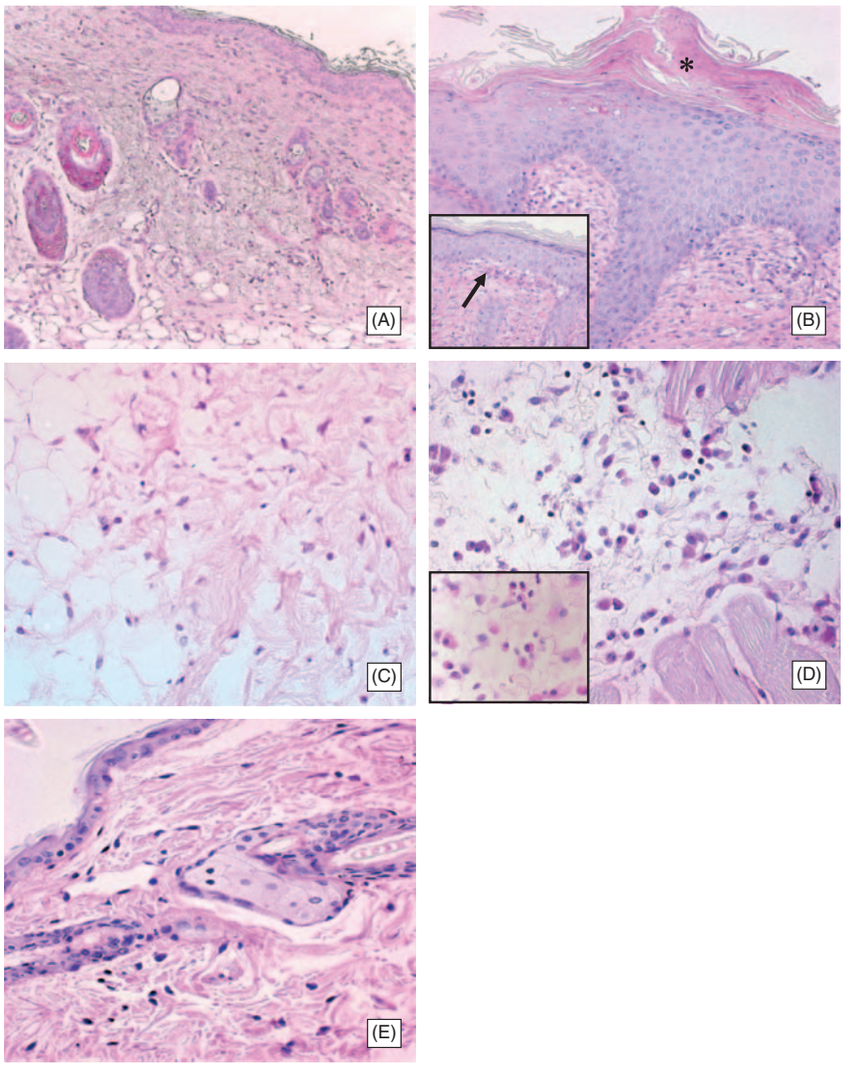

Figure 1 Skin disease in intravenous immunoglobulin (IVIG)-treated (left panels), and saline-treated MRL/lpr mice (right panels) (periodic acid-Schiff [PAS] staining). Hyper- and parakeratosis (asterisk) (A, B, 200×) with excessive stratum spinosum thickening and infiltrating mononuclear cells. Inset: basement membrane in IVIG-treated mice (400×) thickening and vacuoles (arrow). Subcutaneous area without inflammation (C) or inflammatory infiltration with high number of plasma cells (D, 200×; inset: 1000×, PAS). Normal skin of an NMRI mouse (E, 400×) with 1–3 layers of stratum spinosum, a single layer stratum corneum, and the presence of sweat-glands with no sign of inflammation.

Table 2 Renal pathology (microscopic scores) of intravenous immunoglobulin (IVIG)- and saline-treated MRL/lpr mice (mean ± SD)

	IVIG (n = *8*)	*Saline* (n = *10*)	p-*values*
Glomerular cellularity	1.96 ± 0.5	2.19 ± 0.38	0.296
Arteritis	0.723 ± 0.24	0.729 ± 0.44	0.974
Glomerular fibrosis (%)	2.2 ± 3.2	3.15 ± 1.78	0.468

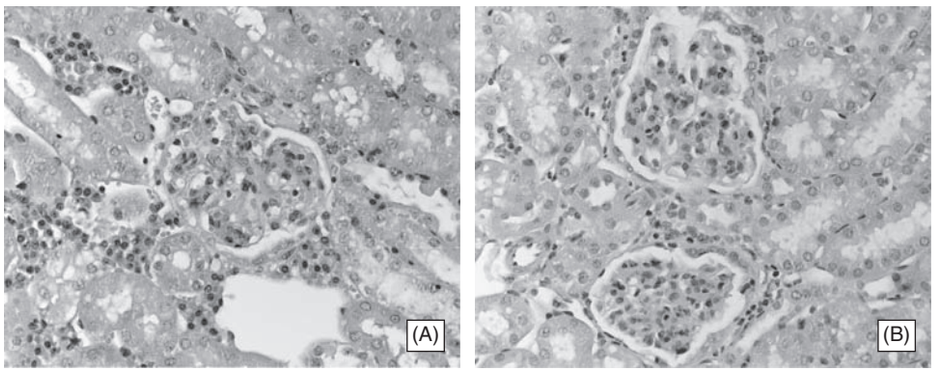

Figure 2 Glomerular changes in intravenous immunoglobulin (IVIG)- (A, moderate glomerular hypercellularity) and saline-treated (B, mild hypercellularity) MRL/lpr mice (hematoxylin and eosin [H&E], 400×).

Furthermore, lymph nodes in control mice were generally enlarged at harvest, while those of IVIG-treated mice were fewer in number and smaller in size (data not shown).

Glomerular damage was not significantly affected by treatment

Untreated MRL/lpr mice developed proliferative lupus nephritis with hypercellularity, dominated by glomerular mesangial cells and mononuclear inflammatory cells, accompanied by hyaline deposition in the glomeruli leading to glomerulocapillary obstruction. Hypercellularity, the extent of hyaline deposition and the ratio of obstructed glomerular capillaries were similar between saline-treated control and IVIG-treated mice (Table 2 and Figure 2).

Retention of blood urea nitrogen demonstrated deterioration of glomerular filtration to a similar extent in both groups suggesting that high-dose, long-term, glycine-stabilized IVIG treatment did not influence renal function in our mouse model (Table 2).

Tubulointerstitial changes

Recruitment of inflammatory cells (plasma cells, lymphocytes) into the tubulointerstitium was also observed in both groups. The extent of inflammatory invasion varied between individual specimens but did not differ significantly between the two groups. Interstitial arteritis and tubular damage (tubulitis, tubular atrophy) were also similar between the groups (Tables 2 and 3). Signs of acute inflammation (tubular necrosis, tubulitis with excess of inflammatory cells and consequential destroyed tubular epithelium) were observed in the tubules of both IVIG- and saline-treated mice.

Table 3 Renal function (blood urea nitrogen) of intravenous immunoglobulin (IVIG)- and saline-treated MRL/lpr mice, and sucrose or maltose treated and untreated NMRI mice (mean ± SD)

Treatment	*Urea (mg/dl)*
IVIG (MRL/lpr)	103.2 ± 63.6
Saline (MRL/lpr)	84.8 ± 22.2
5% sucrose (three times)	47.4 ± 2.1
20% sucrose (once)	64.3 ± 4.03
10% maltose (three times)	53.2 ± 6.0
20% maltose (once)	65.2 ± 14.5
40% maltose (once)	60.8 ± 5.1
No treatment (NMRI)	39.26 ± 4.1

At the time of harvest, the most striking picture of tubular pathology was tubular necrosis. Epithelial cell swelling, loss of brush border and loss of nuclear staining were the most commonly observed changes (Figure 3C–F.) without significant difference between the two groups

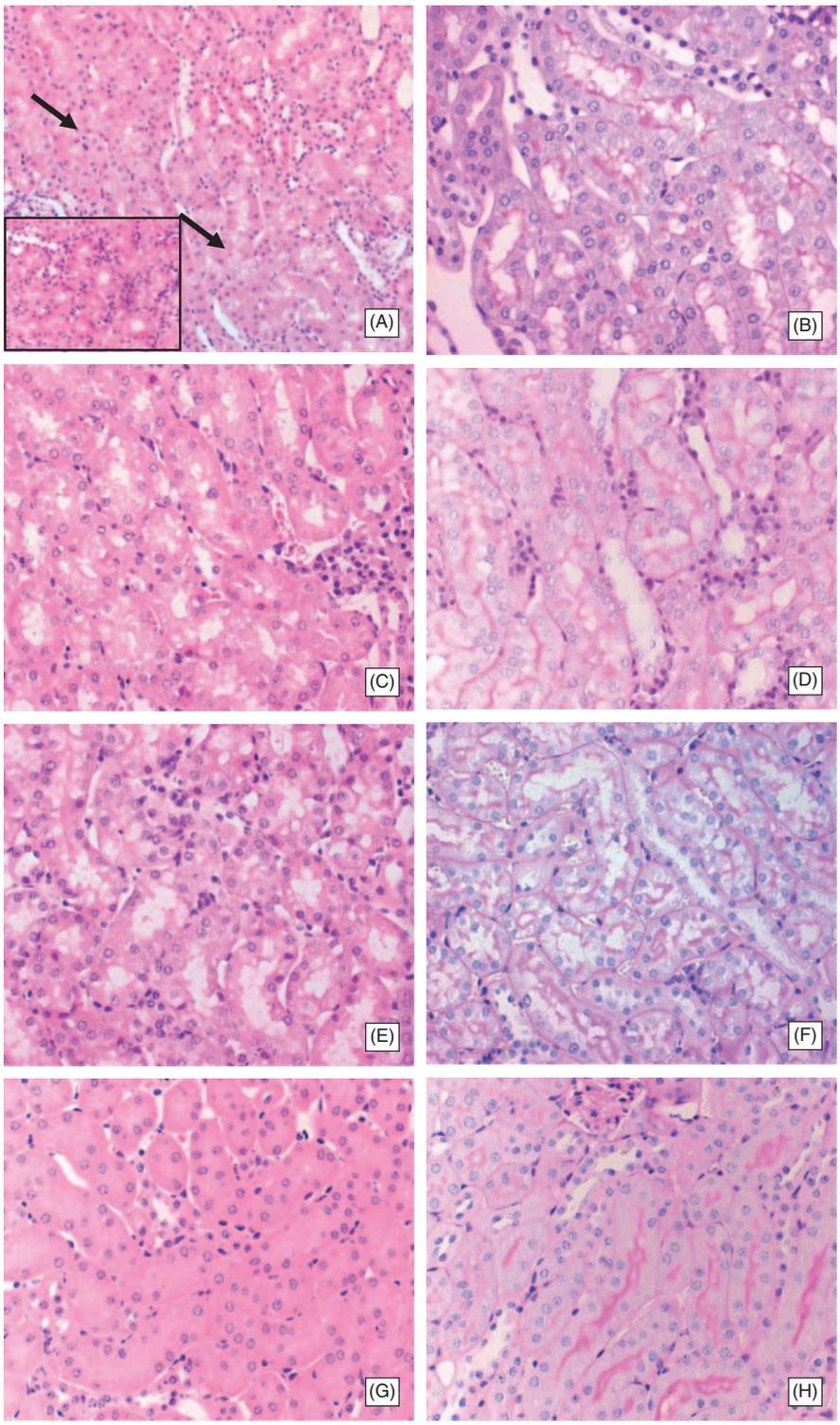

Figure 3 Renal pathology in MRL/lpr and NMRI mice. Hematoxylin and eosin (H&E) staining (right column) and periodic acid-Schiff (PAS) staining (left column). In NMRI mice sucrose-induced hydropic degeneration (arrows, H&E) of tubular cells after three injections of 5% sucrose (A, 200×, H&E; B, PAS, 400×). Inset: sieve-like trellis of vacuoles typical of hydropic degeneration (H&E, 400×). Tubular necrosis without hydropic vacuolization in intravenous immunoglobulin (IVIG)- (C, 400×, H&E; D, 400×, PAS) and saline-treated MRL/lpr mice (E, 400× , H&E; F, 400×, PAS). Normal histologic structure of the kidney of an NMRI mouse (G, 400×, H&E; H, 400×, PAS) with preserved integrity of brush border, tubular epithelial cell, and tubular basement membrane.

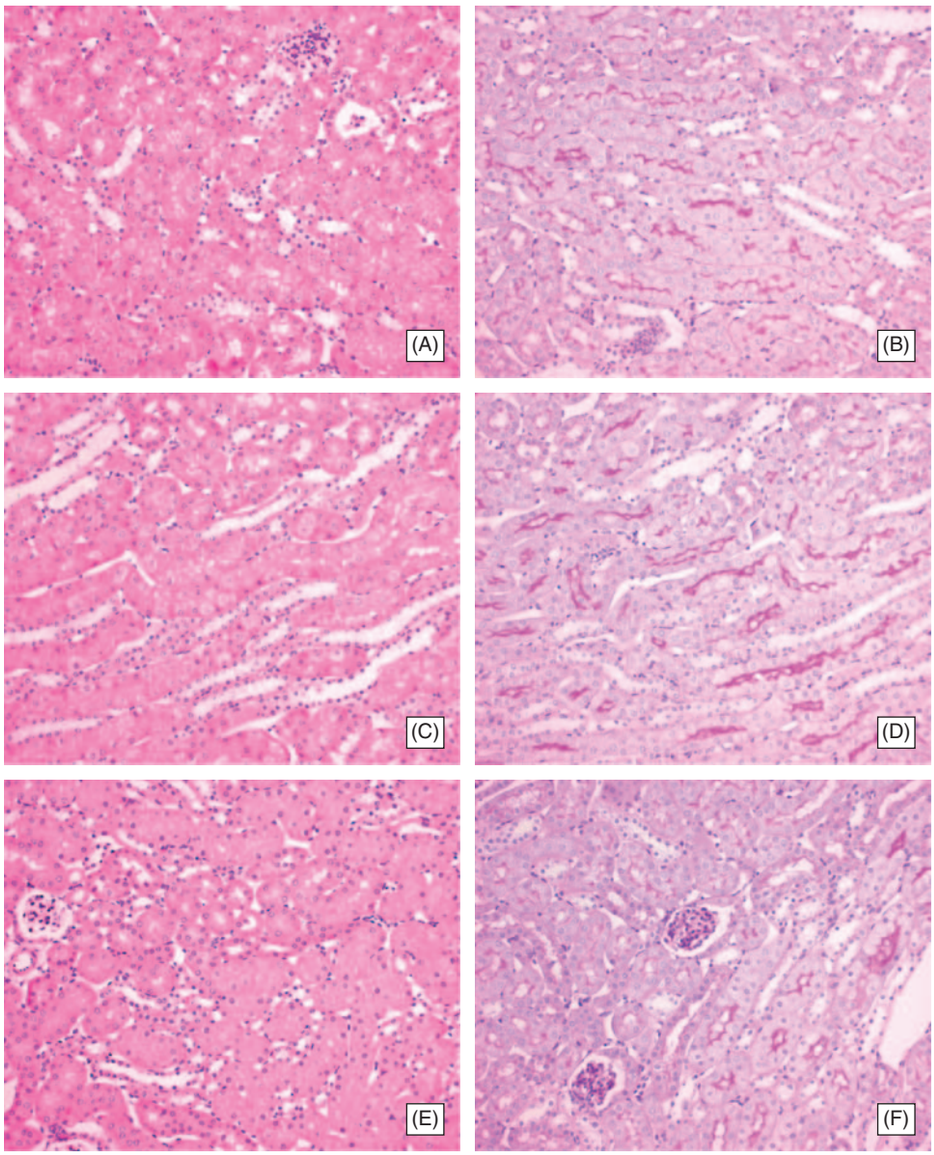

Figure 4 In NMRI mice maltose-induced vacuolar degeneration of tubular cells (right column: hematoxylin and eosin [H&E]; left column: periodic acid-Schiff [PAS]; 200×) after three injections of 10% maltose (A, B), a single injection of 20% maltose (C, D) or 40% maltose (E, F) solution.

(2.42 ± 0.33 versus 2.22 ± 0.446, $p = 0.269$). Interstitial fibrosis as assessed on Mallory's tri-chrome stained kidney specimen was not seen in any of the groups. Fibrosis rarely occurred in score 3 vascular and glomerular damage (Figure 4).

Most commonly, venulitis and low-grade arteritis was seen with perivenular and periarteriolar leukocytic infiltration in both groups of 5-month-old MRL/lpr mice. Vascular inflammation did not differ significantly between the two groups (Table 2).

Hydropic degeneration

Lesions in sucrose-treated positive control kidneys were localized focally to the proximal nephron and consisted of swelling of the tubular epithelium by a fine sieve-like trellis of vacuoles, regularly distributed within the cytoplasm. No typical signs of osmotic nephrosis were present in IVIG- and saline-treated MRL/lpr mice compared with the positive control, 5% sucrose-treated kidneys (Figure 5). Overall renal score was 4.358 ± 1.48 (IVIG) versus 4.76 ± 1.11 (saline), $p = 0.536$.

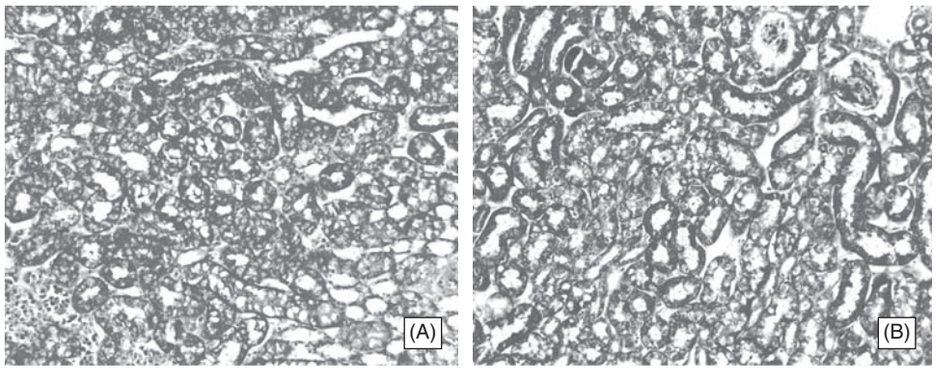

Figure 5 No sign of interstitial fibrosis was seen in (A) intravenous immunoglobulin (IVIG)- and (B) saline-treated MRL/lpr mice after long-term IVIG therapy (Mallory's tri-chrome, 200×).

In maltose-treated positive control mice vacuolar degeneration was observed with mild to severe cellular swelling and presence of eosinophilic epithelial cells. The severity of these changes was dose dependent (Figure 4). Plasma urea levels of maltose- or sucrose-treated mice were between normal and lupus prone mice. The highest urea values were measured in 20% sucrose- and 20% maltose-treated animals. The lowest renal function loss was observed in 10% maltose-treated mice, the analogue of maltose concentration in commercial IVIG preparations (Table 3).

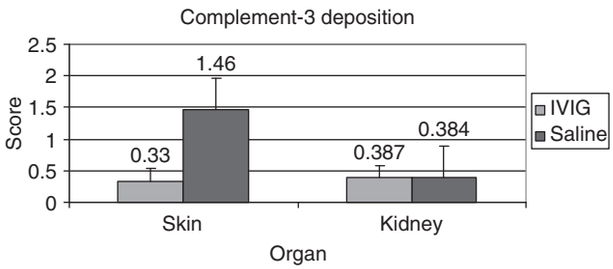

Figure 6 Total scores of complement-3 deposition in skin and kidney of intravenous immunoglobulin (IVIG)- and saline-treated MRL/lpr mice.

Dermal and renal complement-3 deposition

Complement-3 (C3) deposition was observed in the skin on vessel endothelial cells (mainly in the arteries). IVIG treatment diminished C3 deposition in the skin (Figures 6 and 7, $p = 0.02$). In contrast, renal C3 positivity was similar in IVIG- and saline-treated mice (0.387 ± 0.289 versus 0.384 ± 0.267, $p = 0.975$). C3 positivity was present in the glomerular tuft and sometimes within the proximal tubular epithelial cells and tubulointerstitial vessels.

IVIG treatment did not affect plasma autoantibody levels in MRL/lpr mice

Optical density of anti-Sm, anti-DNA and anti-histone autoantibodies were similar in both groups of mice. Positivity for anti-nuclear antibody (ANA) was also observed at the same ratio in IVIG- and saline-treated groups (Table 5). ANA pattern was also similar: mostly homogenous (IVIG: 6, saline: 5), with granular appearance in a few samples (IVIG: 3, saline: 4) in both groups.

Discussion

IVIG therapy of chronic autoimmune inflammatory diseases has been widely investigated[53,54] as it is a rational, safe and possibly beneficial therapy. Despite therapeutic achievements in SLE, rare renal complications contraindicated IVIG therapy. After IVIG nephrotoxicity was attributed to the sugar component of IVIG preparations, IVIG formulations have been changed, and presently glycine is used instead of sucrose, although sugar (sucrose, glucose, maltose)-stabilized IVIG preparations are still available.[55] Our present data demonstrate that glycine-stabilized IVIG has a significant beneficial effect on cutaneous lupus and does not deteriorate lupus nephritis in a high-dose, long-term therapy in a mouse model.

Similarly to our study, the alleviation of skin disease of SLE patients after IVIG therapy has been demonstrated by Gaedicke *et al.*[56] and Ballow and Parke.[57]

In lupus nephritis, IVIG has been considered as a double-edged sword. The fear of ARF restricted

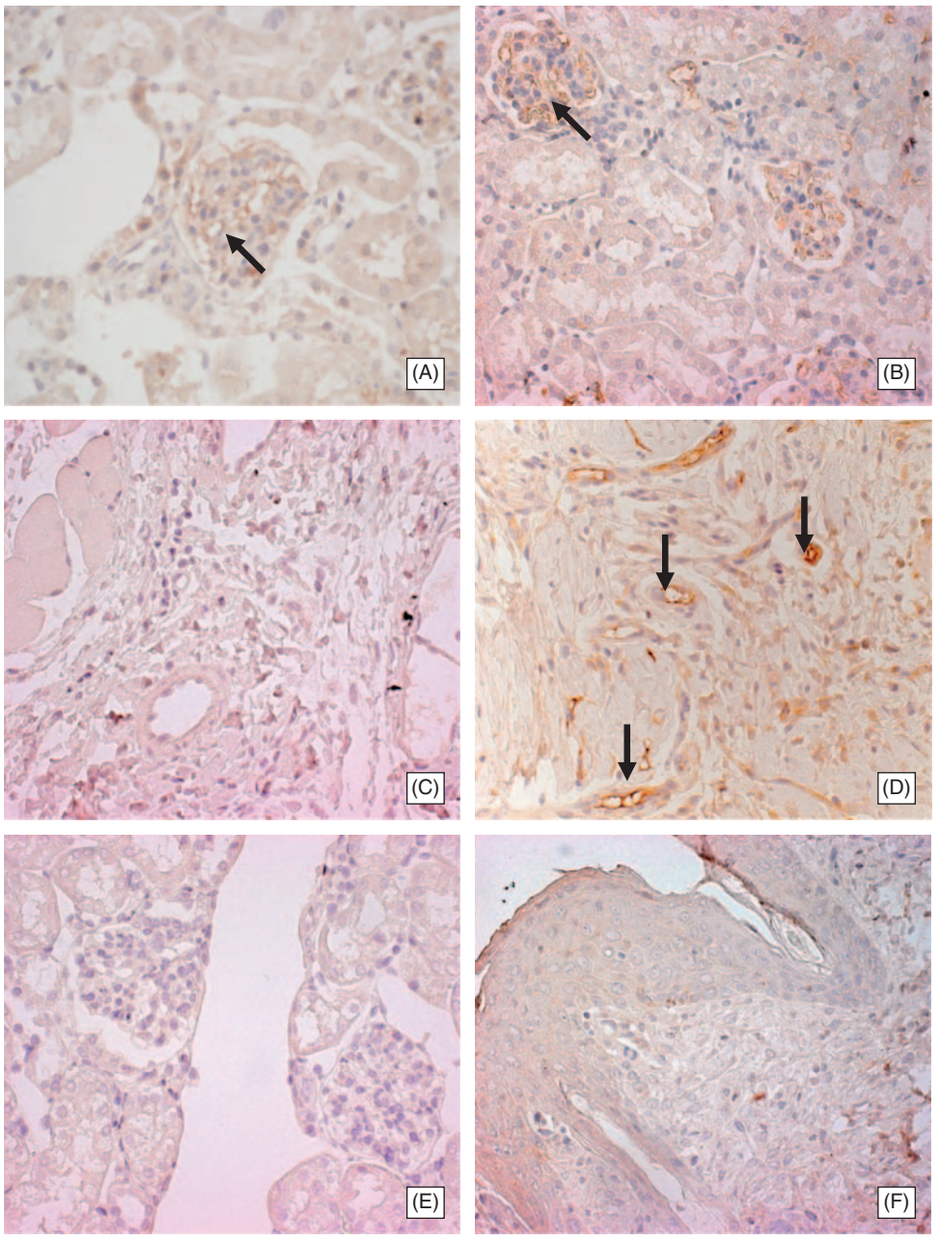

Figure 7 Complement-3 (C3) immunostained kidney (A, B) and skin (C, D) specimen: glomeruli after IVIG (right column) and saline (left column) treatment of MRL/lpr mice (400×). Arrows are pointing at C3-positivity. Negative controls: NMRI mouse kidney (E, 400×) and skin (F, 200×).

Table 4 Tubulointerstitial changes: microscopic scores (numbers represent the number of cases with positive pathology) in intravenous immunoglobulin (IVIG)- and saline-treated MRL/lpr mice

	IVIG (n = *8*)	*Saline* (n = *10*)
Hyaline droplet	2	2
Tubulitis	3	2
Tubular atrophy	1	0
Presence of plasma cells	2	1

Table 5 Lupus autoantibody panel of intravenous immunoglobulin (IVIG)- and saline-treated MRL/lpr mice compared with untreated negative control (NMRI) mice at harvest (mean ± SD of optical density [OD]). Statistics: $p < 0.05$ MRL/lpr groups (IVIG- or saline-treated) versus NMRI, ns: IVIG- versus saline-treated MRL/lpr

Group	*Anti-Sm*	*Anti-DNA*	*Anti-histone*	*Anti-nuclear Ab*
IVIG (MRL/lpr)	3.7 ± 0.2	3.7 ± 0.2	1.9 ± 1.1	2.8 ± 1.0
Saline (MRL/lpr)	3.8 ± 1.7	3.6 ± 0.3	1.4 ± 0.7	3.0 ± 1.5
NMRI	0.01 ± 0.1	0.1 ± 0.02	0.02 ± 0.01	Negative

IVIG use in lupus, despite several reports on the beneficial IVIG effect on lupus nephritis (reduction of proteinuria, stabilization of renal function and histopathological reversal of active lesions).[25,30,33] In our mouse model, lupus nephritis was not affected significantly by long-term IVIG therapy: blood urea nitrogen level and histopathological manifestations of renal damage were similar in IVIG- and saline-treated mice. In accordance with a previous finding,[46] we have also demonstrated that high-dose, long-term therapy with glycine-stabilized IVIG did not induce osmotic nephrosis.

Administration of allogeneic IgG has been shown to induce glomerulonephritis in mice.[58] However, we have not seen any worsening of renal function (blood urea levels) or histology corresponding to glomerulonephritis in IVIG-treated mice compared with saline-treated animals, suggesting that the applied dose and duration did not induce nephritis.

Furthermore, recently maltose-stabilized IVIG has also been introduced to the market, to circumvent sucrose-related nephrotoxicity. However, there are some reports describing the occurrence of ARF after maltose-based IVIG with histologic changes corresponding to osmotic nephrosis. Chacko *et al.*[59] and Metallidis *et al.*[60] reported recently on the cases of lupus nephritis patients who developed ARF after maltose-containing IVIG therapy. These findings can be explained by our study, where vacuolar degeneration developed dose dependently after maltose treatment.

Regarding initiation of IVIG treatment in our model, autoantibody production may begin as early as 6–8 weeks of age in MRL/lpr mice. Our aim was to initiate treatment before the development of already manifest and possibly irreversible organ damage such as skin scarring, or renal damage.[3] Thus, we have initiated IVIG therapy in 6-week-old mice.

The complement system is thought to play an important role in skin lupus, and deposits of C3 were found also in biopsies from clinically normal skin of patients with SLE,[61] suggesting that complement deposition may precede clinical manifestation of skin lupus. It has also been demonstrated that complement inhibition protected against complement-induced vasculitic lesions, but did not affect anti-dsDNA antibody levels and circulating immune complex levels even increased in mice.[62]

The exact mechanisms of complement activation in lupus nephritis are not completely understood. C3-containing immune deposition is an established feature of lupus glomerulonephritis.[63] Although, deficiency of some complement components, such as Factor B[64] may protect against lupus nephritis, deficiency of others (C1q, C4, C2) are associated with lupus in humans and mice.

Glomerular lesions of MRL/lpr mice are mainly associated with immunoglobulin deposits.[65] Diverse manifestations of lupus nephritis have been explained by differences in local expression of endothelial adhesion molecules[66] and different nephritogenic antibodies.[67] Sekine and colleagues demonstrated that C3 knockout MRL/lpr mice developed greater albuminuria and glomerular IgG deposition than heterozygous and wild-type mice. The authors concluded that C3 activation is not essential for full onset of immune complex renal disease.[68] The activation of the alternative pathway is also supposed to play a role in lupus nephritis; since homozygous complement factor B-knockout MRL/lpr mice developed significantly less proteinuria, glomerular IgG deposition, histopathological changes despite normal serum C3 levels.[69] In our long-term IVIG therapy C3-positivity in the kidney was not different between the two groups suggesting that IVIG affects the complement system differently in skin and kidney.

Despite the fact that high-dose IVIG is used as a therapy for SLE, the mechanism(s) of the beneficial effects of IVIG therapy and how it affects autoantibody levels remain poorly understood. It has been hypothesized, that IVIG saturates Fc receptors, resulting in enhanced clearance of endogenous autoantibodies.[70] Furthermore, large amounts of human gamma-globulin could solubilize glomerular IgG deposits,[71] or anti-idiotypic antibodies (anti-Id) in the IVIG preparation may neutralize pathogenic autoantibodies.[72,73] However, IVIG therapy based on anti-idiotypic reaction may require patient specific anti-Ids.[74] In our study, high-dose, long-term IVIG therapy did not reduce autoantibody production in MRL/lpr mice. A possible explanation could be that human IVIG with human anti-Ids might not react with mouse autoantibodies. Thus, the observed differences between skin and kidney effects of IVIG therapy could not be explained by autoantibody removal. However, IVIG is well known to modulate complement activity. High-dose IVIG scavenges fluid phase C3a and C5a[75] both in vitro and in vivo, and competes directly for nascent C3b.[76] C3 has been shown to be responsible in tissue damage which can be reduced by IVIG therapy. In our long-term IVIG therapy C3-positivity was reduced only in the skin suggesting that complement involvement may be different in skin and kidney disease in the MRL/lpr mouse.

Thus, we propose that in our model human IVIG did not affect the measured autoantibodies in MRL/lpr mice, but the beneficial effects of IVIG therapy on skin lupus have been achieved through complement binding.

In conclusion, protection of the skin but not the kidney by glycine-stabilized IVIG therapy suggests divergent pathomechanisms of cutaneous lupus and lupus nephritis. Differential involvement of the complement system may explain the observed differential effects of IVIG therapy. Thus, SLE pathomechanism may not be as uniform, as thought previously. The positive disease-modifying effects of glycine-stabilized IVIG open new doors to clinical therapy of SLE.

Methods

Mice

MRL/lpr (MRL/MpJ-*fas*^{Tnfsrlpr}, MHC haplotype: H2:k) male mice (Jackson Laboratories, USA) were kept under specific pathogen-free conditions in filter-topped cages in an individually ventilated cage system (Charles River Ltd, Budapest, Hungary) and had access to standard rodent chow (Altromin, Lage, Germany) and water ad libitum. Animals were housed four to a cage in both groups to provide a similar social environment. Only littermates were housed together. Body weight was measured weekly.

Treatments

To investigate possible side-effects of long-term, high-dose IVIG therapy, animals were treated once a week from 6 weeks of age until termination of the experiment at the age of 5 months (10 treatments) with immunoglobulin solution stabilized by 10% glycine (Bayer Gamimune N, 10%, Leverkusen, Germany) in a dose of 0.2 ml (0.02 g)/10 g bodyweight, administered into the lateral tail vein. Compared with a high-dose human IVIG injection (400 mg/kg) our mice received 2000 mg/kg.

Mice were anaesthetized with diethyl–ether, body weight was measured and IVIG ($n = 8$) or physiological saline ($n = 10$) (sterile Salsol A infusion, 308 mOsm/l, HUMAN, Gödöllő , Hungary) was injected into one of the side tail veins of mice, which was previously dilated by immersing the tail of the animal into hot water (52–55°C) for a maximum of 5 seconds. After injection, the needle was kept in position for a few seconds before removal, and compression was applied to the tail for haemostasis for a further minute.

To investigate the effect of sugar (sucrose- or maltose-) stabilized IVIG preparations non-lupus prone NMRI mice were injected with 5% sucrose or 10% maltose solution (universal sucrose or maltose content of IVIG preparations) on 3 consecutive days similarly to the protocol used for IVIG injections. Positive controls were also obtained by a single, intravenous administration of 20% sucrose or 20% or 40% maltose into the tail veins of NMRI mice as described elsewhere.[77]

All animal protocols were approved by the Semmelweis University Office of Animal Welfare

Harvest

All animals were sacrificed at the age of 5 months under pentobarbital anaesthesia: intraperitoneal injection of 1% Nembutal (10%, Phylaxia-Sanofi, Budapest, Hungary) supplemented with Heparin (Heparin Biochemie, 500 U/ml, Biochemie GmbH, Kundl, Austria). Bodyweight was measured and the hair of the mice was removed in the interscapular region for observation of the severity of lupus skin disease. Approximately 1 ml blood was obtained from the retroorbital plexus by using heparinized capillaries and plasma was immediately separated by centrifugation at 1000 rpm/10 min/4°C. To remove blood from the tissues, mice were perfused with 4°C Hank's Buffered Salt Solution (HBSS) (w/o Ca, Mg, Gibco, Budapest, Hungary). Perfusion fluid and blood was let out from the circulation through a cut on the vena cava. Interscapular skin and kidney cortex and medulla were removed separately for further examinations.

In order to assess renal function blood urea nitrogen (BUN; mg/dl) levels were measured in a Reflotron Plus laboratory machine with enzymatic reagents (Boehringer Mannheim, Mannheim, Germany) from blood samples obtained by retro-orbital puncture at harvest; 100 µl fractions of sera were snap frozen in liquid nitrogen and stored at –80°C.

Histology

Small pieces (0.5 cm × 0.5 cm) of skin and kidney were snap frozen in OCT compound (Surgipath Medical Inc., Richmond, IL, USA) or fixed in paraformaldehyde (4.5%, phosphate buffered, Semmelweis University Pharmacy, Budapest, Hungary) for a day and then were dehydrated and embedded in paraffin. Sections 4–6 µm thick were deparaffinized, rehydrated and stained consecutively with H&E, periodic acid-Schiff (PAS), or

Table 6 Skin scoring system: (A) macroscopic; (B) microscopic

(A) Observation	0	1	2	3
Interscapular region	No cutaneous lesions	Mild scab, no hair loss	Severe lesions	Extensive ulcerations and ear involvement
Ears	No lesion	Hyperaemia	Scars on less than half of the ear surface	Extensive scarring on more than half of the ear surface
(B) Observation	**Magnification**	**0**	**1**	**2**
Hyper-/parakeratosis	200×	Normal	Mild/moderate (keratin thickness = epidermis)	Severe(keratin thickness > epidermis)
Acanthosis	200×	Maximally 3–5 cell layers/stratum spinosum	Moderate thickening	Disappearance of 'cobble-stone' pattern of stratum spinosum
Basement membrane (BM)	400×	Normal BM	Moderate thickening, vacuolization	Extreme vacuolization, thickening, eosinophilic deposits, membrane tortuosity
Dermal changes	200×	Normal	Moderate thickening	Massive eosinophilic deposits.
Inflammation	200×	No inflammation	Moderate sc. Inflammation	Massive inflammation

Table 7 Renal microscopic scoring system

Observation	*Magnification*	*0*	*1*	*2*	*3*
Glomerular cellularity	400×	Normal	Mild	Moderate	Severe
Capillary obstruction	400×	Open capillaries	In up to one-third of glomeruli	Affecting one-third to two-thirds of glomeruli	Complete in more than two-thirds of glomeruli
Tubulointerstitial (mononuclear) inflammation	200×	Normal	Mild (perivenular and periglomerular)	Moderate (invasion into peritubular areas)	Severe (peritubular, periglomerular and perivenular)
Tubular necrosis	400×	Normal	Tubular swelling, brush border + nuclear loss in less than one-third of tubuli	Nuclear loss in one-third to two-thirds of tubuli	Nuclear loss in more than two-thirds of tubuli
Vascular changes	200×	Normal	Endothelitis	Lymphocytic invasion of tunica muscularis	Transmural lesions/ fibrinoid necrosis
Inflammation	200×	Normal	Moderate sc. inflammation	Massive inflammation	

Mallory's tri-chrome. Samples were examined in a blinded fashion.

Macroscopic and microscopic evaluation

Evaluation of cutaneous lupus on the back of the neck (interscapular region), the ears and the nose was carried out both macroscopically at the time of harvest and microscopically. A macroscopic score for interscapular skin and ears is detailed in Table 6A.

Microscopic scores were evaluated with a Leica DC500 microscope using different magnifications. All photomicrographs were taken with the same microscope.

Hyperkeratosis (expansion of keratin in the epidermis) acanthosis (thickening of stratum spinosum), changes of the basement membrane (thickening, vacuolization, eosinophilic deposits and membrane tortuosity), dermal changes (eosinophilic deposits between collagen bundles and thickening of the dermis), invasion of inflammatory cells (lymphocytes, plasma cells) were evaluated according to the scores listed in Table 6B.

Glomerular cellularity (the extent of inflammatory cell infiltration into the glomeruli, mesangial proliferation and consequent capillary obstruction), perivascular and tubulointerstitial inflammatory cell accumulation (the amount of inflammatory cells surrounding subcortical, periglomerular and peritubular arteries and in the tubulointerstitial area), tubular necrosis (10 cortical fields were randomly scored using a method described by Chetterjee *et al.*[78]), vascular changes (cortical and periglomerular medium-sized renal arteries) were evaluated according to the scores listed in Table 6. Tubulointerstitial fibrosis was assessed in Mallory's tri-chrome stained slides. Hydropic degeneration of tubular epithelial cells was assessed in H&E and PAS stained slides at

400× magnification. The total score of each kidney was calculated by addition of all scores within a sample.

Immunohistological analysis

C3 deposition was evaluated in paraffin-embedded kidney sections using immunohistochemistry as described elsewhere.[79] Briefly, approximately 5 μm thick tissue slices were fixed in ice-cold acetone for 10 minutes then deparaffinized and rehydrated in Tris buffered saline (TBS). Endogenous peroxidase activity was blocked with 3% H_2O_2 (in methanol) for 30 minutes with 5% bovine serum albumin (BSA). Goat anti-mouse C3 (1:200) primary antibody (Cappel Laboratories, Cochranville, PA, USA) was applied for 60 minutes at room temperature dissolved in blocking solution. Samples were incubated with secondary rabbit anti-goat IgG-peroxidase antibody (Sigma-Aldrich, Budapest, Hungary) for 30 minutes in 1:200 dilution. After two washes in TBS (2×5 min), antigen-antibody reaction was developed by 3,3'-diaminobenzidine (DAB) chromogen. Slides were counterstained with Mayer's Hemalaun for 5 minutes, washed in tap water and covered with mounting medium. Glomerular staining was evaluated in a blinded manner at 600× magnification by counting 30 glomeruli per sample, with a semiquantitative score system: 0 = no staining; 1 = weak/<50% staining; 2 = moderate staining in >50% of glomerular tuft. C3 deposition within the skin was observed in capillaries and was counted in each field of view at 200× magnification.

Measurement of lupus autoantibody panel

Anti-Smiths (Sm), anti-double stranded DNA (dsDNA) and anti-histone (H) antibodies were qualitatively measured by commercial enzyme-linked immunosorbent assay (ELISA, Orgentec, Mainz, Germany) according to the manufacturer's instructions. As detection antibody, horseradish peroxidase (HRP) conjugated anti-mouse IgG (Sigma-Aldrich, St Louis, MO, USA) was used (1:1000 dilution in PBS, 1% Tween, 1% BSA). The cut-off value for each ELISA was determined by testing sera of 12 healthy mice. Data are given as average OD ± SD.

ANA were determined by indirect immunofluorescence (IIF) using Hep-2 cells as substrate (The Binding Site, UK), according to the manufacturer's instructions. As detection antibody FITC-conjugated anti-mouse IgG was used (Sigma-Aldrich, St Louis, MO, USA). Sera of 12 healthy mice were tested in parallel as negative controls. A semiquantitative scoring was applied: a 0 value was given for negative samples, 1 for slight positivity in low dilution (1:40) only, 2 for strong positivity in low dilution (1:40) only, 3 for positivity in both low and high (1:80) dilution, and 4 for strong positivity in both low and high dilution. Data are given as average semiquantitative score ± SD.

Statistical analyses

Data are expressed as mean ± SD. All comparisons between groups were made using the Mann–Whitney *U*-test. Differences of $p < 0.05$ were considered statistically significant.

Acknowledgements

The corresponding author declares no competing interests on behalf of all authors. P Hamar was supported by the Hungarian Research Fund (OTKA NF69278, T049022) and a Bolyai fellowship (BO/00351/06). Pathologic scoring was developed with the help of pathologists Dr Kardos Magdolna (Semmelweis Medical University, Institute of Pathology, Budapest), Dr Lipták Péter (Medical University, Szeged) and Dr Degrell Péter (2nd Department of Medicine and Nephrological Center, University of Pecs, Pecs, Hungary).

References

1 Danchenko N, Satia JA, Anthony MS. Epidemiology of systemic lupus erythematosus: a comparison of worldwide disease burden. *Lupus* 2006; 15: 308–318.
2 Holers VM. Anti-C1q autoantibodies amplify pathogenic complement activation in systemic lupus erythematosus. *J Clin Invest* 2004; 114: 616–619.
3 Kökény G, Godó M, Nagy E, *et al*. Skin disease is prevented but nephritis is accelerated by multiple pregnancies in autoimmune MRL/LPR mice. *Lupus* 2007; 16: 465–477.
4 Nicoletti F, Di Marco R, Zaccone P, *et al*. Dichotomic effects of IFN-g on the development of systemic lupus erythematosus-like syndrome in MRL-lpr/lpr mice. *Eur J Immunol* 2000; 30: 438–447.
5 Tokano Y, Morimoto S, Amano HM, *et al*. The relationship between initial clinical manifestation and long-term prognosis of patients with systemic lupus erythematosus. *Mod Rheumatol* 2005; 15: 275–282.
6 Theofilopoulos AN, Dixon FJ. Immune complexes in human diseases. *Am J Pathol* 1980; 100: 529–594.
7 Pizarro S, Monárrez Espino J, Ruiz A, *et al*. Soluble vascular cell adhesion molecule-1 indicates SLE disease activity and specific organ involvement. *Rev Alerg Mex* 2007; 54: 189–195.

8 Tesar V, Masek Z, Rychlik I, *et al*. Cytokines and adhesion molecules in renal vasculitis and lupus nephritis. *Nephrol Dial Transplant* 1998; 13: 1662–1667.
9 Frijns R, Fijnheer R, Schiel A, *et al*. Persistent increase in plasma thrombomodulin in patients with a history of lupus nephritis: endothelial cell activation markers. *J Rheum* 2001; 28: 514–519.
10 Harari OA, Marshall D, McHale JF, *et al*. Limited endothelial E- and P-selectin expression in MRL/lpr lupus-prone mice. *Rheum* 2001; 40: 889–895.
11 Rubinstein T, Pitashiny M, Putterman C. The novel role of neutrophil gelatinase-B associated lipocalin (NGAL)/Lipocalin-2 as a biomarker for lupus nephritis. *Autoimmun Rev* 2008; 3: 229–234.
12 Yang JQ, Saxena V, Xu H, *et al*. Repeated α-galactosylceramide administration results in expansion of NK T cells and alleviates inflammatory dermatitis in MRL-lpr/lpr mice. *J Immunol* 2003; 171: 4439–4446.
13 Carlsten H, Nilsson N, Jonsson R, *et al*. Estrogen accelerates immune complex glomerulonephritis but ameliorates T cell-mediated vasculitis and sialadenitis in autoimmune MRL6lpr mice. *Cell Immunol* 1992; 144: 190–202.
14 Yokoyama H, Kreft B, Kelley VR. Biphasic increase in circulating and renal TNF-alpha in MRL-lpr mice with a differing regulatory mechanism. *Kid Internat* 1995; 47: 122–130.
15 Kikawada E, Lenda DM, Kelley VR. IL-12 deficiency in MRL-Faslpr mice delays nephritis and intrarenal IFN-γ expression, and diminisches systemic pathology. *J Immunol* 2003; 170: 3915–3925.
16 Mitchell DA, Pickering MC, Warren J, *et al*. C1q deficiency and autoimmunity: the effects o genetic background on disease expression. *J Immunol* 2002; 37: 111–123.
17 Yang JQ, Chun T, Liu H, *et al*. CD1d deficiency exacerbates inflammatory dermatitis in MRL-lpr/*lpr* mice. *Eur J Immunol* 2004; 34: 1723–1732.
18 Chan OT, Paliwal V, McNiff JM, *et al*. Deficiency in beta(2)-microglobulin, but not CD1, accelerates spontaneous lupus skin disease while inhibiting nephritis in MRL-Fas(lpr) nice: an example of disease regulation at the organ level. *J Immunol* 2001; 167: 2985–2990.
19 Wuthrich RP, Yui MA, Mazoujian G, *et al*. Enhanced MHC class II (reactive with CD4 T-cells) expression in renal proximal tubules precedes loss of renal function in MRL/lpr mice with lupus nephritis. *Am J Pathol* 1989; 134: 45–51.
20 Suzuka H, Yoshifusa H, Nakamura Y, *et al*. Morphological analysis of autoimmune disease in MRL-lpr, Yaa male mice with rapidly progressive systemic lupus erythematosus. *Autoimmunity* 1993; 14: 275–282.
21 D'Cruz DP, Hughes GRV. The treatment of lupus nephritis. *BMJ* 2005; 330: 377–378.
22 Kaveri SV, Dietrich G, Hurez V, Kazatchkine MD. Intravenuous immunoglobulins (IVIg) in the treatment of autoimmune diseases. *Clin Exp Immunol* 1990; 86: 192–198.
23 Mouthon L, Kaveri SV, Spalter SH, *et al*. Mechanisms of action of intravenous immune globulin in immune-mediated diseases. *Clin Exp Immunol* 1996; 104: S3–S9.
24 Generau T, Chosidow O, Danel C, *et al*. High-dose intravenous immunglobulin in cutaneous lupus erythematosus. *Arch Dermatol* 1999; 135: 1124–1125.
25 Winder A, Molad Y, Ostfeld I, *et al*. Treatment of systemic lupus erythematosus by prolonged administration of high dose intravenous immunoglobulin: report of 2 cases. *J Rheumatol* 1993; 3: 495–498.
26 Levy Y, Sherer Y, Ahmed A, *et al*. A study of 20 SLE patients with intravenous immunoglobulin-clinical and serologic response. *Lupus* 1999; 8: 705–712.
27 Corvetta A, Della Bitta R, Gabrielli A, *et al*. Use of high-dose intravenous immunoglobulin in systemic lupus erythematosus: report of three cases. *Clin Exp Rheumatol* 1989; 3: 295–299.
28 Lafferty TE, Smith JB, Schuster SJ, *et al*. Treatment of acquired factor VIII inhibitor using intravenous immunoglobulin in two patients with systemic lupus erythematosus. *Arthritis Rheum* 1997; 4: 775–778.
29 Sherer Y, Levy Y, Langevitz P, *et al*. Successful treatment of systemic lupus erythematosus cerebritis with intravenous immunoglobulin. *Clin Rheumatol* 1999; 18: 170–173.
30 Boletis JN, Ioannidis JPA, Boki KA, *et al*. Intravenous immunoglobulin compared with cyclophosphamide for proliferative lupus nephritis. *The Lancet* 1999; 354: 569–570.
31 Lin CY, Hsu HC, Chiang H. Improvement of histological and immunological change in steroid and immunosuppressive drug-resistant lupus nephritis by high-dose intravenous gamma globulin. *Nephron* 1989; 53: 303–310.
32 Tan E, Hajinazarian M, Bay W, *et al*. Acute renal failure resulting from intravenous immunolgobulin therapy. *Arch Neurol* 1993; 50: 137–139.
33 Monova D, Belovezhdov N, Altunkova I, *et al*. Intravenous immunoglobulin G in the treatment of pateints with chronic glomeruloneohritis: clinical experience lasting 15 years. *Nephron* 2002; 90: 262–266.
34 Orbach H, Tishler M, Shoenfeld Y. Intravenous immunoglobulin and the kidney—a two-edged sword. *Sem Arthritis Rheum* 2004; 34: 593–601.
35 Barton JC, Herrera GA, Galla JH, *et al*. Acute cryoglobulinemic renal failure after intravenous infusion of gamma globulin. *Am J Med* 1987; 82: 624–629.
36 Wajanaponsan N, Cheng SF. Acute renal failure resulting from intravenous immunoglobulin therapy. *Hawaii Med J* 2004; 63: 266–267.
37 Sati HIA, Ahya R, Watson HG. Incidence and associations of acute renal failure complicating high-dose intravenous immunoglobulin therapy. *Br J Haematol* 2001; 113: 556–557.
38 Fakhouri F. Intravenous immunoglobulins and acute renal failure: mechanism and prevention. *Rev Med Interne* 2007; 28: 4–6.
39 Allen AC (ed.), *The kidney*. *Medical and surgical diseases*. New York: Grune and Stratton; 1951.
40 Cantu TG, Hoehn-Saric EW, Burgess KM, *et al*. Acute renal failure associated with immunoglobulin therapy. *Am J Kidney Dis* 1995; 2: 228–234.
41 Ahsan N, Wiegand LA, Abendroth CS, *et al*. Acute renal failure following immunglobulin therapy. *Am J Nephrol* 1996; 16: 532–536.
42 Haskin JA, Warner DJ, Blank DU. Acute renal failure after large doses of intravenous immune globulin. *Ann Pharmacother* 1999; 33: 800–803.
43 Szenczi A, Kardos J, Medgyesi GyA, *et al*. The effect of solvent environment on the conformation and stability of human polyclonal IgG in solution. *Biologicals* 2005; 34: 5–14.
44 Vo AA, Cam V, Toyoda M, *et al*. Safety and adverse events profiles of intravenuous gammaglobulin products used for immunomodulation: a single-center experience. *Clin J Am Soc Nephrol* 2006; 1: 844–852.
45 Chapman SA, Pham D. Acute renal failure and intravenous immune globulin: occurs with sucrose-stabilized, but not with D-sorbitol–stabilized, formulation. *Ann Pharmacother* 2004; 38: 2059–2067.
46 Hansen-Schmidt S, Silomon J, Keller F. Osmotic nephrosis due to high-dose immunoglobulin therapy containing sucrose (but not with glycine) in a patient with immunoglobulin A nephritis. *Am J Kidney Dis* 1996; 3: 451–453.
47 Cohen PL, Eisenberg RA. Lpr and gld: single gene models of systemic autoimmunity and lymphoproliferative disease. *Annu Rev Immunol* 1991; 9: 243–269.
48 Pisetsky DS, McCarty GA, Peters DV. Mechanisms of autoantibody production in autoimmune MRL mice. *J Exp Med* 1980; 152: 1302–1310.
49 Kolaja GJ, Fast PE. Renal lesions in MRL mice. *Vet Pathol* 1982; 19: 663–668.
50 Diaz GC, Jevnikar AM, Brenan DC, *et al*. Autoreactive kidney-infiltrating T-cell clones in murine lupus nephritis. *Kidney Int* 1992; 42: 851–859.
51 Kanauchi H, Furukawa F, Imamura S. Characterization of cutaneous infiltrates in MRL/lpr mice monitored from onset to the full development of lupus erythematosus-like skin lesions. *J Invest Dermatol* 1991; 96: 478–483.

52 Furukawa F, Tanaka H, Sekita K, *et al*. Dermatopathological studies on skin lesions of MRL mice. *Arch Dermatol Res* 1984; 276: 186–194.
53 Gürcan HM, Ahmed AR. Efficacy of various intravenous immunoglobulin therapy protocols in autoimmune and chronic inflammatory disorders. *Ann Pharmacother* 2007; 5: 812–823.
54 Ruetter A, Ludger TA. Efficacy and safety of intravenous immunoglobulin for immune-mediated skin disease: current view. *Am J Clin Dermatol* 2004; 5: 153–160.
55 Medlin Plus. Immune Globulin Intravenous Injection. http://www.nlm.nih.gov/medlineplus/druginfo/meds/a682815.html
56 Gaedicke G, Telle WM, Kohne E, *et al*. IgG therapy in systemic lupus erythematosus. *Annals of Hematology* 1984; 48: 387–390.
57 Ballow M, Parke A. The uses of intavenous immune globuline in collagen vascular disorders. *J Allergy Clin Immunol* 1989; 84: 608–612.
58 Kaneko Y, Nimmerjahn F, Madaio MP, Ravetch JV. Pethology and protection in nephrotoxic nephritis is determined by selective engagement of specific Fc receptors. *JEM* 2006; 203: 789–797.
59 Chacko B, John GT, Balakrishnan N, Kirubakaran MG, Jacob CK. Osmotic nephropathy resulting from maltose-based intravenous immunoglobulin therapy. *Ren Fail* 2006; 28: 193–195.
60 Metallidis S, Papaioannu M, Bokolas G, Kollaras P, Gogou V, Nikolaidis P. Acute renal failure following intravenous immunoglobulin therapy in HIV-infected patient. *Clin Nephrol* 2009; 71: 196–197.
61 Ullman S, Halberg P, Wolf-Jürgensen P. Deposits of immunoglobulins and complement C3 in clinically normal skin of patients with lupus erythematosus. *Acta Derm Venereol* 1975; 55: 109–112.
62 Alexander JJ, Bao L, Jacob A, *et al*. Administration of the soluble complement inhibitor, Crry-Ig, reduces inflammation and aquaporin 4 expression in lupus cerebritis. *Biochim Biophys Acta* 2003; 1639: 169–176.
63 Zabaleta-Lanz ME, Munoz LE, Tapanes FJ, *et al*. Further description of early clinically silent lupus nephritis. *Lupus* 2006; 15: 845–851.
64 Watanabe H, Garnier G, Circolo A, *et al*. Modulation of renal disease in MRL/lpr mice genetically deficient int he alternative complement pathway factor B. *J Immunol* 2000; 164: 786–794.
65 Ito MR, Terasaki S, Kondo E, *et al*. Experimental lupus nephritis is severe combined immunodeficient (SCID) mice: remodelling of the glomerular lesions by bystander IgM antibodies. *Clin Exp Immunol* 2000; 119: 340–345.
66 Nakatani K, Fujii H, Hasegawa H, *et al*. Endothelial adhesion molecules in glomerular lesions: association with their severity and diversity in lupus models. *Kidney Int* 2004; 65: 1290–1300.
67 Itoh J, Nose M, Takahashi S, *et al*. Induction of different types of glomerulonephritis by monoclonal antibodies derived from an MRL/lpr lupus mouse. *Am J Pathol* 1993; 143: 1436–1443.
68 Sekine H, Reilly CM, Molano ID, *et al*. Complement component C3 is not required for full expression of immune complex glomerulonephritis in MRL/lpr mice. *J Immunol* 2001; 166: 6444–6451.
69 XXX.
70 Bleeker WK, Teeling JL, Hack CE. Accelerated autoantibody clearance by intravenous immunoglobulin therapy: studies in experimental models to determine the magnitude and time course of the effect. *Blood* 2001; 98: 3136–3142.
71 Tomino Y, Sakai H, Takaya M, Suga T, Endoh M, Nomoto Y. Solubilization of intraglomerular deposits of IgG immune complexes by human sera or gamma-globulin in patients with lupus nephritis. *Clin Exp Immunol* 1984; 58: 42–48.
72 Blank M, Manosroi J, Tomer Y, *et al*. Suppression of experimental systemic lupus erythematosus (SLE) with specific anti-idiotypicantibody-saporin conjugate. *Clin Exp Immunol* 1994; 98: 434–441.
73 Tomer Y, Shoenfeld Y. Successful treatment of psychosis secondary to SLE with high-dose intravenous immunoglobulin. *Clin Exp Rheumatol* 1992; 10: 391–393.
74 Bakimer R, Gilburd B, Zurgil N, Shoenfeld Y. The effect of intravenous-γ-globulin on the induction of experimental antiphospholipid syndrome. *Clin Exp Immunopathol* 1993; 69: 97–102.
75 Basta M, Van Goor F, Luccioli S, *et al*. F(ab)'2-mediated neutralization of C3a and C5a anaphylatoxins: a novel effector function of immunoglobulins. *Nat Med* 2003; 9: 431–438.
76 Berger M, Rosenkranz P, Brown CY. Intravenous and standard immune serum globulin preparations interfere with uptake of ^{125}I-C3 onto sensitized erythrocytes and inhibit hemolytic complement activity. *Clin Immunol Immunopathol* 1985; 34: 227–236.
77 Wilmer HA. The mechanism of sucrose damage of the kidney tubules. *Am J Physiol* 1944; 141: 431–438.
78 Chetterjee PK, Cuzzocrea S, Brown PAJ, *et al*. Tempol, a membrane-permeable radical scavenger, reduces oxidant stress-mediated renal dysfunction and injury in the rat. *Kidney Int* 2000; 58: 658–673.
79 Girardi G, Berman J, Redecha P, *et al*. Complement C5a receptors and neutrophils mediate fetal injury in the antiphospholipid syndrome. *J Clin Invest* 2003; 112: 1644–1654.